Bioconjugate Chemistry

Article

pubs.acs.org/bc

Improved Catalyzed Reporter Deposition, iCARD

Jesper Lohse,* Kenneth Heesche Petersen, Nina Claire Woller, Hans Christian Pedersen, Galina Skladtchikova, and Rikke Malene Jørgensen

Dako A/S, Produktionsvej 42, 2600 Glostrup, Denmark

Supporting Information

ABSTRACT: Novel reporters have been synthesized with extended hydrophilic linkers that in combination with polymerizing cross-linkers result in very efficient reporter deposition. By utilizing antibodies to stain HER2 proteins in a cell line model it is demonstrated that the method is highly specific and sensitive with virtually no background. The detection of HER2 proteins in tissue was used to visualize individual antigens as small dots visible in a microscope. Image analysis-assisted counting of fluorescent or colored dots allowed assessment of relative protein levels in tissue. Taken together, we have developed novel reporters that improve the CARD method allowing highly sensitive *in situ* detection of proteins in tissue. Our findings suggest that *in situ* protein quantification in biological samples can be performed by object recognition and enumeration of dots, rather than intensity-based fluorescent or colorimetric assays.

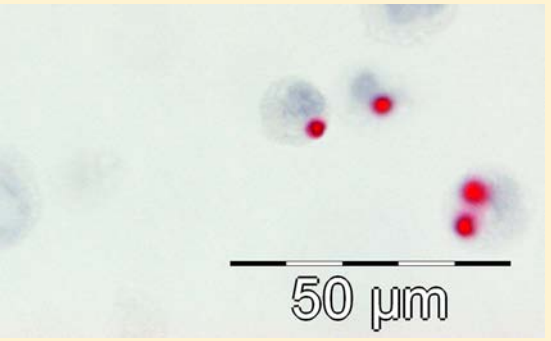

INTRODUCTION

Detection of immobilized proteins in formalin fixed paraffin embedded tissue biopsies is known as immunohistochemistry (IHC).[1] A typical procedure starts with high temperature protein target retrieval of a 4−5 μm thin section of embedded sample on microscope slides, followed by incubation with a primary antibody specific for the protein being assayed. This antibody is then recognized in a second step with horseradish peroxidase (HRP)-labeled secondary antibody, followed by deposition of diaminobenzidine (DAB) and counterstaining of cell nuclei with hematoxilin. This produces a dark brown end-product in sites of protein expression in combination with blue cell nuclei, allowing interpretation of the resulting protein stains in the context of cellular morphology. As an alternative to HRP and DAB, alkaline phosphatase (AP)-labeled antibody conjugates may be used to produce, e.g., red stains, either as stand alone or in double stains in combination with DAB.

For many proteins the standard IHC method works well.[2] However, the sensitivity of the method is too low for detection of target proteins expressed in very low amounts and the semiquantitative nature of the method poses serious challenges. Even trained human observers have difficulties assessing the degree of brown staining as demonstrated by a number of reports on intra- and interinterpreter variability with unacceptable levels of false positives and false negatives.[3,4] Assays where the diagnostic IHC result is decisive for patient treatment (pharmacodiagnostics assays) would in particular benefit from a true quantitative assessment of protein levels as opposed to the existing semiquantitative intensity-based IHC method.[5,6] Increased precision of the IHC assay in a clinical study setting would enable ease of interpretation and establishment of cutoff values. Thus, the need exists for methods allowing more sensitive, objective, and quantitative detection of immobilized proteins.

The catalyzed reporter deposition system (CARD) addresses the limited sensitivity of IHC by introducing an extra layer of enzymatic amplification.[7] Rather than depositing DAB, the HRP enzymes can be used to deposit reporters comprising a phenol and a detectable label such as fluorescein isothiocyanate (FITC) or biotin. In the next step, the labels are recognized by another layer of HRP- or AP-labeled antibodies or avidins, followed by the final dye deposition. The mechanism is based on oxidation of the phenol part of the reporter by HRP into highly reactive radicals that react with aromatic amino acids at sites of HRP activity.[7] As many different reporters have been prepared and are commercially available, the method is very versatile. Low abundance proteins,[8] DNA, RNA[9] and fluorescence multistains[10] are among today's applications.

Reporters are typically prepared from a fluorescent compound via reaction with tyramine, 4-(2-aminoethyl)-phenol, to produce tyramides. Tyramides have the limitation that low concentrations (80 μM) have to be used in order to promote reaction with the tissue rather than reporter dimerization.[11] Tyramine dimers are soluble in water and are thus not deposited.

To overcome this limitation and increase the efficiency of the CARD system, we speculated that addition of a cross-linking co-substrate to the deposition reaction mixture might enhance reporter deposition. We initially focused on DAB since the HRP-mediated polymerization of DAB leads to insoluble

Received: July 9, 2013
Revised: May 2, 2014
Published: May 11, 2014

dx.doi.org/10.1021/bc400311g | *Bioconjugate Chem.* 2014, 25, 1036−1042

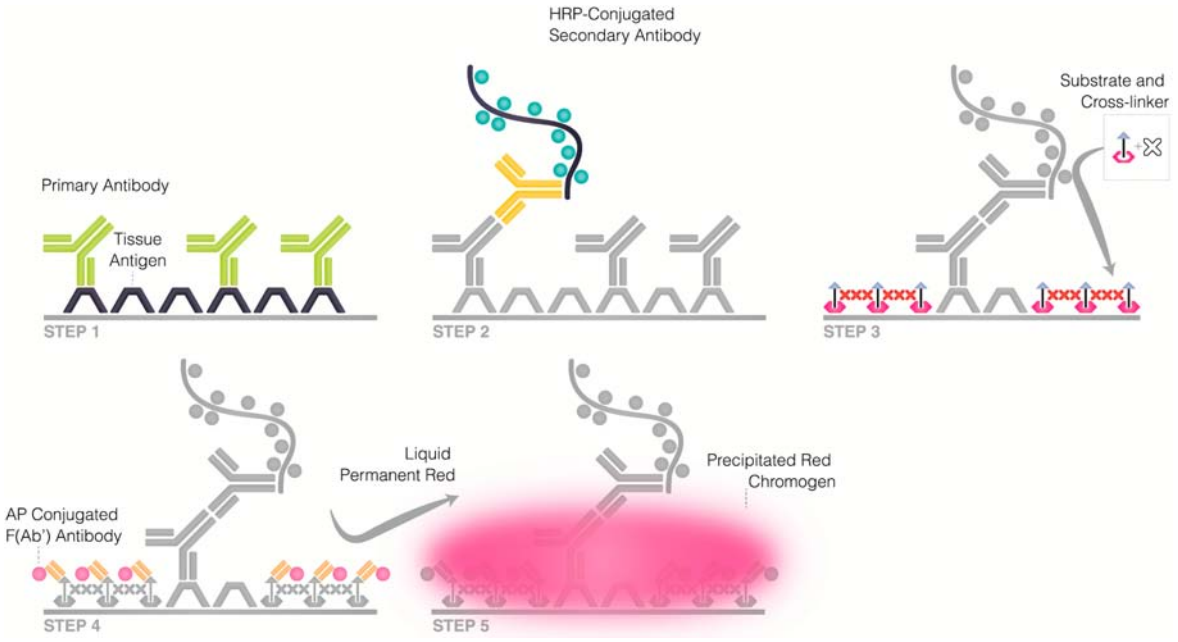

Figure 1. Improved catalyzed reporter deposition (iCARD) system. First an antibody is bound to antigens in the sample (Step 1). Next a secondary antibody−enzyme dextran conjugate is used to recognize the primary antibody (Step 2). Enzyme substrate and cross-linker are precipitated around the antigen by the enzymes (Step 3). Recognition of the antigen attached to the enzyme substrate with an enzyme/antibody conjugate (Step 4). Finally, a chromogen precipitation gives dots in the desired color (Step 5).

deposits, providing reporters with abundant aromatic anchoring grounds as alternative to dimerization (see Figure 1).

RESULTS AND DISCUSSION

Reporter Design. To avoid quenching of fluorescent labels by the cross-linking DAB deposits and to enhance accessibility of labels to further enzymatic amplification steps, reporters with extended hydrophilic linkers were prepared using solid phase chemistry. Orthogonally protected lysine residues were used for attachment of labels and HRP substrates either on solid phase or following cleavage from solid support. This allowed the preparation of diverse reporters with different linker length and varying numbers of labels and HRP substrates (see Table 1 and Figure 2). Rather than tyramine or similar simple phenols, ferulic and cinnamic acids were built into the reporters to serve as HRP substrates. These hydroxy-cinnamic acid derivatives are among HRPs natural substrates.[12] High turnover rate constants have been reported for HRP-mediated oxidation of ferulic acid.[13]

Initial optimization experiments confirmed that addition of DAB to the deposition reaction mixture did indeed boost deposition efficiency considerably, and secondary antibody−HRP conjugates could be used in high dilution, yet still produced intense stains. With further optimization, the stains exhibited a grainy appearance, and at extreme dilutions of the conjugates, distinct small dots were produced. We speculated that each dot originated from individual molecules of antibody conjugate. If each conjugate was attached to a single protein through a primary antibody, then enumeration of dots could be used as a quantitative measure of protein in the tissue. The number of the most protein molecules in tissue is so high that if every protein should be visualized with a ~4 μm^2 dot, the result would be a complete staining of the tissue similar to a standard IHC staining. For the purpose of counting proteins, the conjugate was diluted to an extent where the conjugate, via the primary antibody, only labels a small fraction of the proteins present. Thus, rather than assessing the area and intensity of the stain, the number of dots detected in the tissue would reflect the number of available epitopes and thereby target protein levels. If the concentration of conjugate is kept constant, the number of dots will vary with the target protein

Table 1. Table of Reporters[a]

reporter	molecular weight calculated, (found)	N-terminal HRP substrates	spacer	label on C-terminal lysine side chain
1	3446(3447)	Fer-Lys(Fer)-	L150	Carboxy-Fluorescein
2	3751(3752)	Fer((Lys(Fer))$_2$	L150	Carboxy-Fluorescein
3	4055(4054)	Fer((Lys(Fer))$_3$	L150	Carboxy-Fluorescein
4	4360(4359)	Fer((Lys(Fer))$_4$	L150	Carboxy-Fluorescein
5	2273(2271)	Fer((Lys(Fer))$_2$	L60	Carboxy-Fluorescein
6	6303(6302)	Sin((Lys(Sin))$_2$	L300	Carboxy-Fluorescein
7	1780(1779)	Fer((Lys(Fer))$_2$	L30	Carboxy-Fluorescein
8	4175(4173)	Sin((Lys(Sin))$_3$	L150	Carboxy-Fluorescein
9	3841(3839)	Sin((Lys(Sin))$_2$	L150	Carboxy-Fluorescein
10	3696(3696)	Fer((Lys(Fer))$_3$	L150	NH2 (none, free amino group)
11	3790(3788)	Fer-Lys(Fer)-	L150	Texas RedX
12	3350(3348)	H_2N-((Lys(NH_2))$_3$ (none, free amino groups)	L150	Carboxy-Fluorescein

[a]Fer is ferulic acid, Sin is cinnapinic acid. See Supporting Information for detailed chemical structure.

dx.doi.org/10.1021/bc400311g | Bioconjugate Chem. 2014, 25, 1036−1042

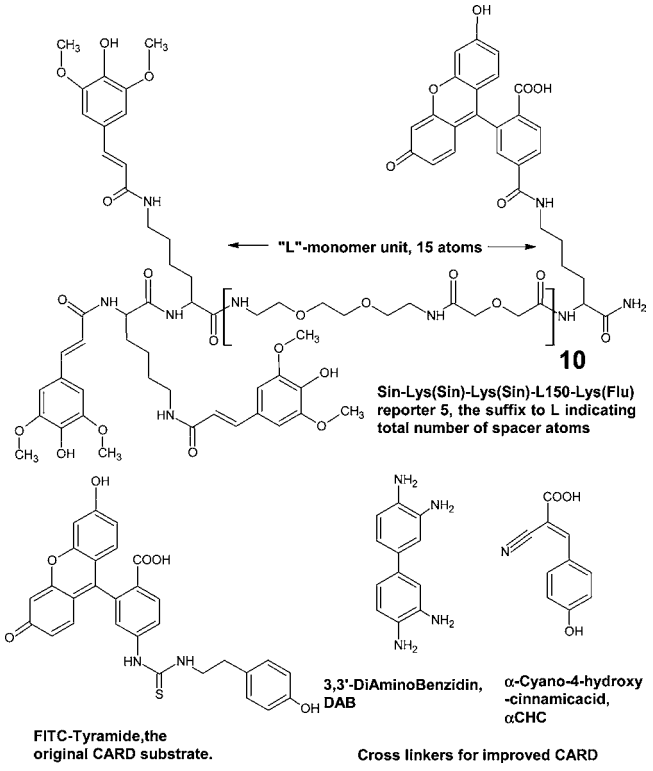

Figure 2. Structure of reporter 5, Sin-Lys(Sin)-Lys(sin)-L150-Lys(Flu), FITC-Tyramide, the original CARD subtrate, and the two cross-linkers DAB and αCHC. Notice that while FITC-Tyramide only has 5 atoms of spacer between fluorescein and a single phenolic HRP substrate, we found that 3–4 HRP substrates and around 150 atoms of spacer is optimal. Both cross-linkers are very reactive and bifunctional with two phenylenediamine moieties, DAB, or a phenol linked to a cyanoacrylate, αCHC.

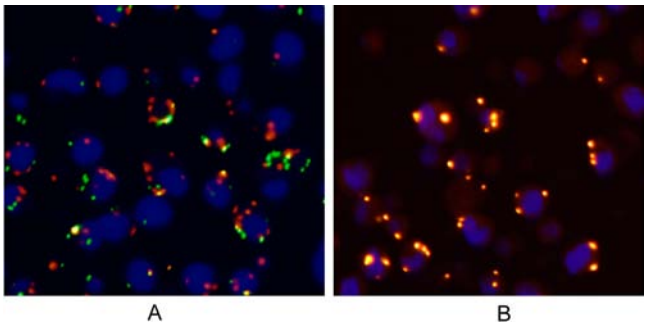

Figure 3. MDA-MB-175 cell line. (A) Stained sequentially with reporter **4** (green) and reporter **11** (red). (B) Stained simultaneously with a mix of reporter **4** and reporter **11**.

Control experiments showed that all the initial fluorescent dots deposited in the first enzymatic amplification step could be converted to colored dots in the second enzymatic amplification step, even following fluorescence image capture (Figure 4A and B). The colored dots appeared larger than the

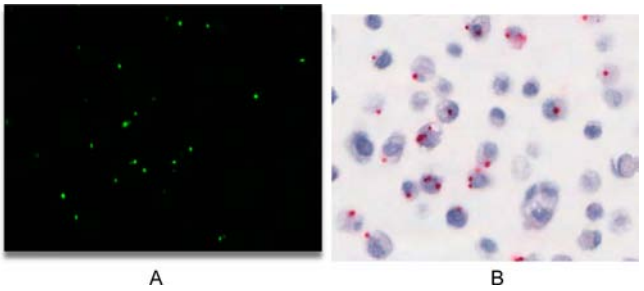

Figure 4. The same section of a single slide with the MDA-MB-175 cell line at different steps of the iCARD protocol. (A) Stopped after the first precipitation of reporter **4** and cross-linker. (B) Continued to include a chromogenic precipitation.

expression level in the tissue as the fraction visualized is kept constant.

To investigate whether the observed dots were indeed derived from single molecules, we carried out a single target, dual-color fluorescence experiment. A cell line with intermediate HER2 target expression level (MDA-MB-175 cells) was incubated with a primary anti-HER2 antibody followed by secondary HRP conjugate. They were first stained as green fluorescent dots with the carboxy-fluorescein-labeled reporter **3** and, following a second incubation with secondary HRP conjugate, the targets were stained as red fluorescent dots with the Texas Red-labeled reporter **11** (Table 1). This resulted in a mixture of individual green and red dots (Figure 3A). A control staining with a single incubation with secondary HRP conjugate followed by a mixture of the two reporters **3** and **11** resulted in uniform yellow dots (Figure 3B). Staining of single target protein molecules would be expected to give rise to either green or red dots if the staining is saturated in the color generating step and is not affected by the subsequent color generating step. Staining of clusters of several molecules, however, would be expected to result in mixed colors from varying degrees of green and red fluorescent deposits. A few yellow areas were in fact observed (Figure 3A), indicating that overlapping of green and red dots can occur, i.e., the first color-generating step does not prevent color generation in the subsequent step. As individual green and red dots were predominantly observed, it is suggested that the dots derive from single molecule targets. fluorescent dots presumably due to additional diffusion of the final dyes. Experiments with extensive washing steps following the reporter deposition step resulted in smaller dots, showing that reporter deposits were only to some extent covalently anchored (results not shown).

Counting Dots. Further experiments demonstrated many advantages associated with large dot size. Essentially all dots could be captured in a single *Z*-plane image at relative low magnification (0.5×0.5 μm^2 pixels) with resulting good resolution of depth and moderate raw image data size. Thus, further optimization focused on generating larger dots. The low background and high roundness minimized detection of false positive dots. Furthermore, in case of dot overlap the intensity gradient from periphery to center aided detection and segregation of overlapping dots by gradient-based algorithms. Concordance in assessment of "Dot" vs "no Dot" between observers and different algorithms was 98–99%.

Optimization of Reporter Structure. A systematic study of spacer length led to optimal reporter design and shed light on the reaction mechanism. Reporters **5** and **7** with short spacers (60 and 30 atoms, respectively) produced smaller dots with background staining than reporter 3 with 150 atoms spacer. Surprisingly, extending the spacer to 300 atoms with reporter **6** resulted in very small dots and much background (results not shown).

dx.doi.org/10.1021/bc400311g | *Bioconjugate Chem.* 2014, 25, 1036–1042

By comparing reporters with identical spacer length and label we found that reporter **3** with four ferulic acid residues produced larger dots than either reporters **1**, **2**, or **4** with two, three, or five residues, respectively. Likewise, reporter **9** with three cinnamic acids produced larger dots than reporter **8** with four residues.

The reaction was also studied directly in solution by addition of HRP to deposition reaction mixtures, followed by MALDI-TOF analysis of the reaction products, a tool exploited by other groups.[12] This showed formation of soluble reporter/DAB adducts consistent with initial radical copolymerization in solution.

We also found that α-cyano-4-hydroxycinnamic acid, a phenolic cyanoacrylate worked well as cross-linker. Based on these findings, we suggest the following reaction mechanism: HRP enzymes catalyze radical chain reaction polymerization of the cross-linker leading to extensive cross-linker deposition and formation of insoluble reporter/cross-linker adducts. These initially precipitate and are to some extent covalently bound to the sample. Balanced water solubility (spacer) and a moderate number of HRP substrates (ferulic acid) seems key to reporter design. Too many HRP substrates lead to lower solubility and smaller localized deposits, whereas few HRP substrates lead to too high solubility and prevent the initial precipitation of reporter/cross-linker adducts.

Optimization of Deposition Reaction Mixture. Starting from a standard 50 mM imidazole:HCl deposition buffer, multiple parameter variation studies were utilized to optimize deposition conditions with regard to concentration of hydrogen peroxide, reporter, cross-linker, pH, and reaction time. Under optimal conditions, both cross-linkers produced almost perfectly round, 5−6 μm^2 dots, in both cases without any perceptible background (see Figure 4).

While some variation in dot size was observed, a histogram of dot size revealed a bell curve with very few small dots close to the lower dot detection limit (see Figure 5). This indicates that not only are single conjugate molecules detected as dots, but it also appears that almost all conjugate molecules produce detectable dots. Indeed, optimization experiments reached a plateau with regard to dot number. Once the average size of the dots exceeded 4 μm^2, further increasing deposition efficiency or incubation time with dyes resulted in larger dots, not to markedly more dots.

With optimized conditions, a direct comparison was made to the original FITC-tyramide CARD system was made. Keeping all other parameters constant, we substituted our deposition mixture with commercially available FITC-tyramide. While this resulted in a dotty staining too, the dots were mostly smaller than 1 μm^2 and significantly fewer dots were observed, suggesting that many conjugates did not produce visible dots with FITC-tyramide.

We also tried addition of DAB and α-cyano-4-hydroxycinnamic acid to the FITC-tyramide precipitation mixture, but in our hands both compounds inhibited the reaction, resulting in even smaller or no dots.

Measure of Cell Line Protein Expression Level. A test system based on cell lines (MDA-MB-231, MDA-MB-175, and SK-BR-3) expressing different levels of target protein HER2 (weak, intermediate, and strong) was used for exploring the quantitative potential of counting dots, as embedded cell lines represent uniform and stable protein expression. Staining of the target HER2 protein and counting of the produced dots in the three different cell lines showed the expected trend in HER2 expression levels. Dot counts reached 1900 (MDA-MB-231), 7400 (MDA-MB-175), and 50 000 (SK-BR-3) with staining of around 20 000 cells (see Table 2). For assessment of the background level, the primary antibody binding to the target HER2 protein was omitted from the assay and replaced by buffer. Only 30−50 dots were detected across the three different cell lines each constituting around 20 000 cells and demonstrated very low background giving an excellent signal-to-noise ratio. After omitting both primary and secondary antibody, the count was down to 0−4 dots per 20 000 cells, representing image analysis noise typically resulting from specks of hematoxilin precipitates.

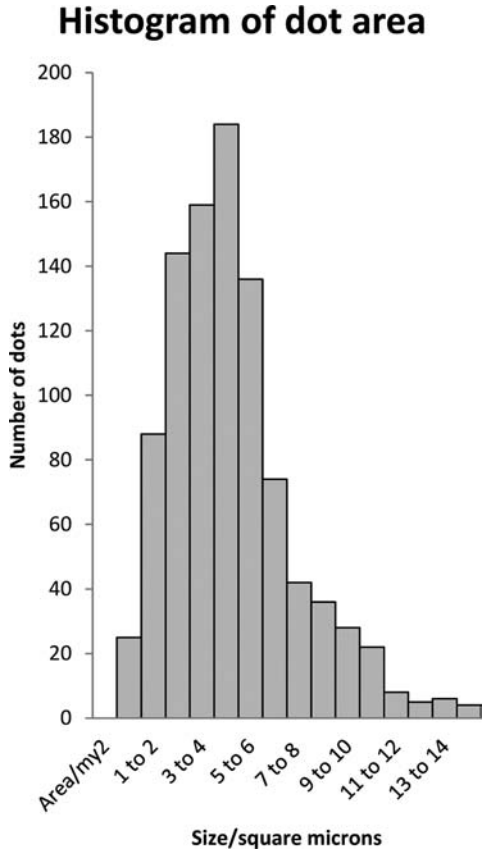

Figure 5. Histogram showing the number of dots with a given size in square micrometers (μm^2).

Table 2. Dots/Cell Across Different Cell Lines[a]

cell line	SK-BR-3	MDA-MB-175	MDA-MB-231
primary and secondary HRP conjugate	2.38 dots/cell	0.37 dots/cell	0.094 dots/cell
secondary HRP conjugate only	0.0026 dots/cell	0.0011 dots/cell	0.0019 dots/cell
signal to noise. (dot/cell with primary/without primary)	915 dots/cell	336 dots/cell	49 dots/cell

[a]Slides were incubated for 20 min with either blocking buffer or 1 μg/mL anti-HER2, followed by 20 min 500 fM secondary HRP conjugate. Each ratio is an average of triple determination.

Dots in Tissue. Tissue sections of breast cancer samples expressing different levels of target protein HER2 were stained using the dot staining protocol developed on cell lines and subsequently stained by a standard IHC method, producing a dual stain of the sample tissue (see Figure 6). The number of

dx.doi.org/10.1021/bc400311g | Bioconjugate Chem. 2014, 25, 1036−1042

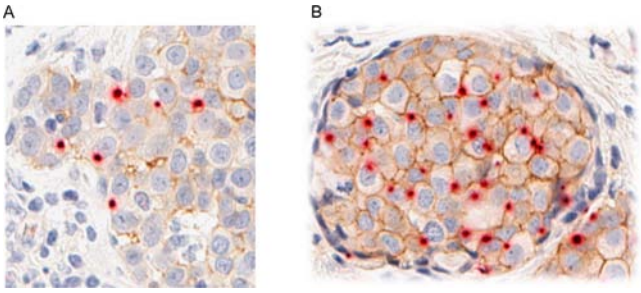

Figure 6. Sections of breast cancer tissue with low (A) or moderate (B) expression of HER2 protein. Sections were first stained with iCARD (red dots) and then with a standard HER2 IHC method (brown DAB deposits).

dots in the two tumor samples (low and intermediate expression of target protein HER2) correlated with the intensity of the deposited standard brown DAB stain of target protein HER2 located on the cell membranes. Most dots were indeed found in the expected target location, i.e., centered on the cell membranes (see Figure 6). The standard DAB stain delineated the cell membranes, and the dots were generally round shaped, not elongated, and aligned with the cell membrane pattern indicating that the dot derived from a single point and not from clusters of HER2 protein stained by multiple antibody conjugates.

We recognize that proving that the dots are derived from single molecules will be difficult. However, the dual color fluorescence experiment, the concordance observed between fluorescence and bright field, the relative homogeneous size and roundness of the dots even in case of membranous targets, and the fact that dot size does not diminish with dilution of the secondary conjugates all indicate that dots are not derived from clusters of target proteins or conjugates.

■ CONCLUSION

The CARD system has significantly been advanced with the use of cross-linkers in combination with novel refined reporter structures in the catalytic enzyme deposition step. The deposition efficiency has been pushed to the extent of creating large dots, to the best of our knowledge, allowing visualization of individual protein targets through antibody binding and subsequent enzyme deposition. Even though only a fraction of the immobilized protein in tissue can be visualized by this technique, it could form the basis for developing a quantitative and objective assay by enumeration of dots by automated image analysis.

Furthermore, this advancement holds the potential of improving the quality level of IHC assays as the dot stains are derived by methods similar to the existing IHC method and can be combined with a standard stain as double stains including counterstain. Ultimately this allows biomarker quantification in combination with full morphological interpretation on the same slide.

■ MATERIALS AND METHODS

Chemical Analysis. MALDI-TOF mass spectra were run in house on a Bruker Autoflex. ^{1}H and ^{13}C NMR analyses were carried out at University of Roskilde on a Varian instrument in DMSO-d_6 solution. Elemental analyses were performed by DB Lab, www.dblab.dk. UV−vis spectra were recorded on a PerkinElmer lambda 35 spectrophotometer. Reporter concentration was determined via carboxyfluorescein absorption at 498 nm using 73 000/M cm as molar coefficient of extinction. Preparative RP-HPLC was performed on a Gilson system on C18 column, and analytical HPLC was carried out on a Waters alliance system on C18 column, in both cases with acetonitrile/water gradient with 0.02% TFA.

Tissue and Control Cell Lines. Breast carcinoma tissues were obtained from Department of Pathology, Odense University Hospital, Denmark, fixed in formaldehyde prior to embedding in paraffin for 24 h. The FFPE tissue blocks were cut in 4 μm sections. All specimens were completely anonymized prior to receipt at Dako. According to the Danish law on the Research Ethics Committee System and handling of biomedical research projects and communication between Dako and the Danish Committee on Biomedical Research Ethics and the Regional Ethics Committee (IRB) the tests performed at Dako on anonymous residual tissue and anonymized blood are not subject to approval by the IRB system because such studies are considered quality control projects. Therefore, no IRB approval for this work has been obtained.

For IHC analysis on cell lines, control slides from HercepTest with the cell lines MDA-MB-231, MDA-MB-175, and SK-BR-3 were used.

Immunohistochemistry. Slides were deparaffinized via baths of 2 × 5 min xylene, 2 × 2 min 96% ethanol, 2 × 2 min 70% ethanol, and finally transferred to demineralized water.

Target retrieval was performed in a buffer of 5 mM Na-Hepes, pH 8.0. Up to 20 slides in 250 mL target retrieval were heated to 100 °C in a microwave oven for 4 min at 750 W, and boiled for 10 min at 350 W and allowed to cool to room temperature (20−25 °C).

Automated staining was performed on an Autostainer Plus (Dako). Polyclonal rabbit anti-HER2 from HercepTest kit was used as primary antibody. Polyclonal goat anti-rabbit conjugated to HRP was used as secondary antibody. Polyclonal rabbit anti-FITC conjugated to calf intestine AP was used as tertiary conjugate to produce colored dots for bright field microscopy. See Supporting Information for protocols for each type of stain.

For fluorescence imaging, the slides were transferred to demineralized water and dehydrated in 99.9% ethanol followed by mounting with VectaShield with DAPI. Fluorescence images were captured on a Leica DM 6000 B with 40× objective and Leica DFC 300FX camera through FITC/Texas Red double filter and DAPI filter.

For bright field imaging, the slides were rinsed with water, dehydrated in 99.9% ethanol, and coverslipped with Sakura Tissue-Tek Film Coverslipper. The images were captured on Aperio ScanScope CS at 20×.

For image analysis of dot size and numbers the software CISH v 1.2 from Indica Laboratories was used. To generate the histogram in Figure 4, data was exported via Excel into the freeware JMicrovision v 1.27.

Synthesis of Reporters. (See Supportive Information for synthesis of Boc-L30-OH.) Example Fer-(Lys(Fer))$_3$-L150-Lys(Flu)-NH$_2$. Reporter 3. Two grams MBHA-resin was downloaded with 10 mL 0.06 M HATU activated Boc-Lys(Fmoc)-OH and capped with 20% acetic anhydride in pyridine/NMP for 1 h. With standard Boc-chemistry, five units of L30 were introduced by coupling with 10 mL 0.26 M HATU activated Boc-L30-OH in NMP for 2 × 20 min, followed by three units of Boc-Lys(2ClZ). The Fmoc-group was removed

with 20% piperidine in NMP for 2 × 10 min, and the C-terminal lysine side chain labeled with 10 mL 0.2 M 5(6)-carboxyfluorescein in NMP activated with HATU and 1.0 equiv DIPEA for 3 × 20 min. The resin was washed with 20% piperidine in NMP, NMP, DCM, and finally acidified with 5% *m*-cresol in TFA. The intermediate product, reporter 12, H-$(Lys(NH_2))_3$-L150-Lys(Flu)-NH_2 was cleaved from the resin with a cleavage cocktail of 9 mL TFA, 3 mL TFMSA, 1.5 mL *m*-cresol, and 1.5 mL thioanisole for 2 h and precipitated by addition of 150 mL diethyl ether. Following two additional precipitations from TFA and one from NMP, the intermediate was dissolved in 10 mL NMP and 1 mL DIPEA. This was mixed with 10 mL 0.2 M ferulic acid in NMP activated with 0.9 equiv HATU and 2 equiv DIPEA for 1 min, and reacted for 10 min. The reaction was quenched by addition of 2 mL ethylenediamine for 2 min and the crude product precipitated with diethyl. Following three additional precipitations from TFA, the product was dissolved in 25% acetonitrile in water and subjected to RP-HPLC purification with an acetonitrile gradient in 0.02% TFA, eluding with 40% acetonitrile. MALDI-TOF and analytical HPLC was used to identify pure fractions that were pooled, neutralized with sodium MES, and freeze−dried. The yield was 875 mg, 0.216 mmol, 36%, and the purity was >99% by HPLC. Using this scheme a number of reporters **1**−**12** were prepared (Table 1).

As an alternative to introducing the label on solid phase the reporter intermediate 10 was prepared: On 1 g MBHA-resin Boc-$(Lys(_2ClZ))_3$-L150-Lys(Fmoc)-NH_2 was prepared as described above. Following cleavage from resin and labeling with ferulic acid in solution and quenching with ethylenediamine, further addition of piperidine led to Fmoc deprotection and allowed isolation of Fer-$(Lys(Fer))_3$-L150-Lys(NH_2)-NH_2. The yield was 177 mg, 0.048 mmol, 24%.

Such intermediates were used to prepare reporters in solution where the label was prohibitively expensive to use in large amounts for solid phase labeling or did not tolerate cleavage conditions from solid phase.

Reporter 11. Fer-Lys(Fer)-L150-Lys(Texas Red X)-NH_2: Fer-Lys(Fer)-L150-Lys(NH_2)-NH_2 was prepared analogously to reporter intermediate 10. 2 μmol was dissolved in 100 μL NMP and 5 μL DIPEA. 5 mg Texas Red X-NHS ester was added and allowed to react for 30 min. The reaction mixture was quenched by addition of 100 μL ethylenediamine for 2 min and the product isolated by precipitation with diethyl ether. It was redissolved in 200 μL TFA, precipitated, and purified by HPLC. The yield was 4 mg, 50%. MALDI-TOF 3791.3, calculated 3790.21 for $C_{169}H_{267}N_{28}O_{65}S_2$, purity by analytical HPLC was 97.4%.

See Figure 2 for chemical structure of reporters and cross-linkers.

■ ASSOCIATED CONTENT

Ⓢ Supporting Information

Details on the chemical synthesis of Boc-L30, and on the immunohistochemistry protocols are provided. This material is available free of charge via the Internet at http://pubs.acs.org.

■ AUTHOR INFORMATION

Corresponding Author

*E-mail: jesper.lohse@dako.com.

Notes

The authors declare no competing financial interest.

■ ACKNOWLEDGMENTS

Helene Derand and Kristian Jensen are thanked for inspiring discussions; Dorte Carlsen, Linda Thejl, Marianne Marcussen, Anne Bruun, and Anne Maarbjerg are thanked for skilled technical assistance.

■ ABBREVIATIONS

CARD, catalyzed reporter deposition; iCARD, improved catalyzed reporter deposition; Fer, ferulic acid; Flu, fluorescein; IHC, immunohistochemistry; HRP, horseradish peroxidase; TFA, trifluoroacetic acid; DAB, diaminobenzidine; FFPE, formalin-fixed, paraffin-embedded; DAPI, 4′,6-diamidino-2-phenylindole; HATU, *O*-(7-azabenzotriazol-1-yl)-*N*,*N*,*N*′,*N*′-tetramethyluronium hexafluorophosphate; NMP, *N*-methyl-2-pyrrolidone; TFMSA, trifluoromethanosulfonic acid; MES, 2-(*N*-morpholino)ethanesulfonic acid; DCM, dichloromethane; MBHA, 4-methylbenzhydrylamine; Sin, sinapinic acid; DIPEA, *N*,*N*-diisopropylethylamine

■ REFERENCES

(1) Dabbs, D. J. (2014) *Diagnostic Immunohistochemistry*, 4th ed., Elsevier.

(2) Mokry, J. (1996) Versatility of immunohistochemical reactions: comprehensive survey of detection systems. *Acta Medica (Hradec Kralove) 39*, 129−140.

(3) Thomson, T. A., Hayes, M. M., Spinelli, J. J., Hilland, E., Sawrenko, C., Phillips, D., Dupuis, B., and Parker, R. L. (2001) HER-2/neu in breast cancer: interobserver variability and performance of immunohistochemistry with 4 antibodies compared with fluorescent in situ hybridization. *Mod. Pathol. 14*, 1079−86.

(4) Walker, R. A. (2006) Quantification of immunohistochemistry–issues concerning methods, utility and semiquantitative assessment I. *Histopathology 49*, 406−10.

(5) Hicks, D. G., and Kulkarni, S. (2008) HER2+ breast cancer: review of biologic relevance and optimal use of diagnostic tools. *Am. J. Clin. Pathol. 129*, 263−73.

(6) Wolff, A. C., Hammond, M. E., Schwartz, J. N., Hagerty, K. L., Allred, D. C., Cote, R. J., Dowsett, M., Fitzgibbons, P. L., Hanna, W. M., Langer, A., McShane, L. M., Paik, S., Pegram, M. D., Perez, E. A., Press, M. F., Rhodes, A., Sturgeon, C., Taube, S. E., Tubbs, R., Vance, G. H., van de Vijver, M., Wheeler, T. M., and Hayes, D. F. (2007) American Society of Clinical Oncology/College of American Pathologists guideline recommendations for human epidermal growth factor receptor 2 testing in breast cancer. *J. Clin. Oncol. 25*, 118−45.

(7) Bobrow, M. N., Harris, T. D., Shaughnessy, K. J., and Litt, G. J. (1989) Catalyzed reporter deposition, a novel method of signal amplification. Application to immunoassays. *J. Immunol. Methods 125*, 279−85.

(8) Hasui, K., and Murata, F. (2005) A new simplified catalyzed signal amplification system for minimizing non-specific staining in tissues with supersensitive immunohistochemistry. *Arch. Histol. Cytol. 68*, 1−17.

(9) Schmidt, B. F., Chao, J., Zhu, Z., DeBiasio, R. L., and Fisher, G. (1997) Signal amplification in the detection of single-copy DNA and RNA by enzyme-catalyzed deposition (CARD) of the novel fluorescent reporter substrate Cy3.29-tyramide. *J. Histochem. Cytochem. 45*, 365−73.

(10) Harigopal, M., Barlow, W. E., Tedeschi, G., Porter, P. L., Yeh, I. T., Haskell, C., Livingston, R., Hortobagyi, G. N., Sledge, G., Shapiro, C., Ingle, J. N., Rimm, D. L., and Hayes, D. F. (2010) Multiplexed assessment of the Southwest Oncology Group-directed Intergroup Breast Cancer Trial S9313 by AQUA shows that both high and low levels of HER2 are associated with poor outcome. *Am. J. Pathol. 176*, 1639−47.

(11) Bobrow, M. N., Shaughnessy, K. J., and Litt, G. J. (1991) Catalyzed reporter deposition, a novel method of signal amplification.

II. Application to membrane immunoassays. *J. Immunol. Methods 137*, 103−12.
(12) Oudgenoeg, G., Dirksen, E., Ingemann, S., Hilhorst, R., Gruppen, H., Boeriu, C. G., Piersma, S. R., van Berkel, W. J., Laane, C., and Voragen, A. G. (2002) Horseradish peroxidase-catalyzed oligomerization of ferulic acid on a template of a tyrosine-containing tripeptide. *J. Biol. Chem. 277*, 21332−40.
(13) Henriksen, A., Smith, A. T., and Gajhede, M. (1999) The structures of the horseradish peroxidase C-ferulic acid complex and the ternary complex with cyanide suggest how peroxidases oxidize small phenolic substrates. *J. Biol. Chem. 274*, 35005−11.